SPE-195319-MS

Revisiting Kelvin Equation for Accurate Modeling of Pore Scale Thermodynamics of Different Solvent Gases

Ilyas Al-Kindi and Tayfun Babadagli, University of Alberta

This paper was prepared for presentation at the SPE Western Regional Meeting held in San Jose, California, USA, 23-26 April 2019.

Abstract

Understanding the thermodynamics of fluids in capillary media is essential to achieve a precise modeling of EOR applications such as hybrid (with thermal methods) and sole solvent injection processes. The theoretically derived classical Kelvin equation describes the influence of surface tension, contact angle, pore radius, and temperature on vapour pressures. The deviation of propane vapour and condensation pressures from this equation was determined experimentally by measuring them on capillary/porous media with various sizes and types, namely Hele-Shaw glass cells, silica-glass microfluidic chips, and rock samples. The experimental data were also compared with the vapour pressures obtained for the bulk conditions. The gap thicknesses in Hele-Shaw cells were 0.13 and 0.04 mm whereas the medium size in micromodels was ranging from 142 to 1μm. The results showed that vapour and condensation pressures of propane recorded in the experiments were comparatively close to the bulk vaporization pressure and calculated vapour pressures from the Kelvin equation. Conversely, vapour pressures obtained from rock samples were noticeably lower than bulk vapour pressures.

Key words: Classical Kelvin equation, capillary media, pore radius, propane vapour pressure

Introduction

Using solvents in heavy-oil recovery has become a common thought since injecting said chemicals solely or as co-injectant with steam can improve oil recoveries. Different types of hydrocarbon and non-hydrocarbon solvents were considered previously due to their effective diffusion capabilities into crude oil and bitumen. Nasr et al. (2003) investigated the impact of co-injecting hydrocarbon solvents (propane to heptane range suggesting hexane as the optimal one) with steam in heavy oil and bitumen recovery during steam assisted gravity drainage (SAGD) operations. The research generally focused on improving oil rate, enhancing oil steam ratio, reducing required energy, and dropping water consumption. The selection criteria of solvents was performed based on vaporization and condensation temperatures, and how close they are to the water vaporization and steam condensation temperatures. Léauté and Carey (2007) studied the impact of C5+ condensate on bitumen recovery in cyclic steam stimulation (CSS) process for the Cold Lake field.

The application was inspected in the field as a pilot project through eight wells that were under CSS operation. It was reported that adding 6% volume fraction of diluent into steam during CSS enhanced the well performance and results were above the expectations.

Utilizing hydrocarbon solvents in heavy-oil recovery applications has a significant limitation due to operational cost. Injecting large volumes of solvents could be expensive and uneconomical in many circumstances depending on oil prices. To minimize the overall application cost, Bahlani and Babadagli (2009) introduced the idea of Steam Over Solvent Injection in Fractured Reservoirs (SOS-FR) to retrieve the trapped solvents in the reservoirs thermally by steam or hot-water injection. The process consists of three main stages: (1) injecting steam to condition the oil by reducing its viscosity, (2) injecting solvent to recover remaining oil through chemical diffusion and gravity segregation, and (3) injecting steam or hot water to retrieve the trapped solvents with remaining oil. According to experimental observations and numerical study, trapped solvents could be recovered up to 80-85% with 85-90% of the original oil in place.

The phase-change is controlled not only by pressure and temperature but also capillary and interfacial characteristics as porous media becomes tighter. This phenomenon leads the vapour pressures and boiling points to deviate from the bulk conditions and this process is controlled by the size of the pores and wettability conditions. To model hybrid or sole-solvent injection precisely under non-isobaric and non-isothermal conditions, actual phase-change behaviours of fluids in various porous media should be well understood through experimental and theoretical investigations.

Studying vapour pressure alteration of propane in extended tight rocks, such as shales, was experimentally performed by Zhong et al. (2018) by using nanofluidic chips featured with silicon nanochannels. The chips had various sizes of channels ranging from 20 μm to 8 nm. Condensation of propane within the confined channels was observed under a range of pressure (~0.6-2.3 MPa) and temperature (286.15-339.15 K). The study also aimed to validate theoretical modelling (Kelvin equation) by comparing calculated results with the experimental outcomes. Vapour pressures, obtained from the Kelvin equation, were closely matching the experimental outcomes even in extended confined channels (~8 nm) making the equation applicable in modelling capillary condensation. Vapour pressure alteration of water in nanochannels was inspected by Tsukahara et al. (2012) using a nanoscale chip. The nanofluidic chip consisted of microchannels (10 μm deep) and nanoscale channels with a depth range of 90-370 nm. The experiments demonstrated the reduction of water vapour pressure with the decrease of medium size. Additionally, computed vapour pressures from the Kelvin equation were relatively similar to those observed in the experiment; therefore, applicability of the Kelvin equation in predicting vapour pressures within extreme confined media was still valid.

The curvature effect on fluids increases as capillary size becomes tighter due to the change of interfacial properties such as surface tension and pressure difference at the liquid-gas interface. Several investigations were performed to understand the deviation of phase-change behaviour in extreme tight channels featured with nanoscale pore throats (Bao et al. 2017). The majority of these studies were conducted using microfluidic and nanofluidic chips made of silica glass. Per the Kelvin equation, the alteration of vapour pressure in confined pores depends on capillary size, surface tension, and contact angle between the solid surface and liquid. These liquid-solid properties, including molecular absorption of the surface, might change noticeably when the solid material is altered. This paper aims to study the phase-change behaviour of propane in various capillary media starting from Hele-Shaw glass cells to real core samples with different permeabilities, porosities, and pore throat sizes. Moreover, microfluidic chips with uniform and non-uniform properties (grain and pore throat sizes) representing various pore sizes were utilized to obtain a clearer picture of propane phase alteration in porous media using visual support. One of the main targets in this investigation was to inspect the effect of surface properties on propane's vaporization and condensation in confined spaces.

Comparative analysis of the outcomes obtained from glass microfluidic experiments and rock samples provided new insight into the pore scale thermodynamics of the solvents to be used in further computational studies to improve the accuracy of performance prediction.

Statement of the Problem and Objectives

In heavy-oil recovery applications, injecting solvents with or without steam under variable pressure and temperature could lead to considerable phase alteration. The thermodynamics of injected fluids in porous media play a critical role in controlling the performance of hybrid and cold-solvent injection. Phase alteration during the process could control the distribution of injected fluids in the reservoir as well as their flow dynamics and eventually, oil recovery. Similarly, solvent retrieval process (SRP) highly depends on solvents thermodynamics in the reservoir. As a result, comprehending the phase-change behaviour of injected fluids is important in choosing the appropriate application conditions (such as pressure and temperature) while maximizing oil recovery and solvent retrieval. In fact, SRP is a critical part of the whole process and has an impact in minimizing the overall operational cost of hybrid (steam-solvent) applications.

The operation becomes more complex and challenging while dealing with heterogeneous reservoirs (fractured carbonates or layered sandstones). Recovering the trapped solvents, in such cases, can be possible by vaporizing them thermally or through pressure depletion process to relocate the trapped solvents from low to high permeability zones. Another common application is unconventional reservoirs where solvents are injected (usually under isothermal conditions) after fracking. The phase change mechanism should be well understood during this process as it directly affects the oil recovery (during injection) and solvent retrieval (during depletion) and the phase behaviour in capillary medium is different from the bulk conditions of which are applied in classical PVT tests and studies.

A similar phenomenon is encountered in oil (heavy-oil, light, oil, and condensate) recovery from unconventional (shales, tight sands) reservoirs in which the most common application suggested is solvent gas (hydrocarbon gases or CO_2). The gases injected (in the form of huff-and-puff) after fracking diffuse into rock matrix and reproduce with oil during the depletion stage. The recovery of oil and solvent retrieval are both controlled by the thermodynamics (mainly the phase change of the solvent and oil). It is well know that the phase change conditions in capillary medium differ from the bulk conditions and this cannot be captured easily using standard PVT analyses.

Per the Young-Laplace equation ($\Delta P = 2\gamma/r$), the curvature radius (r) has an effect on surface tension (γ) when it decreases to microscales or nanoscales (Tsukahara et al., 2012). The Kelvin equation demonstrates the relationship between vapour pressures in capillary and bulk conditions ($P_r = P_\infty \exp\left[\frac{2\,\sigma\,v^L}{r\,R\,T}\right]$). According to this equation, vapour pressure of fluids becomes lower than those in bulk scenarios when medium sizes are tighter due to the change of surface tension, pressure drop at the interface, and contact angle. As a result, fluids in highly confined spaces tend to have higher viscosities and capillary pressures. This phenomena is highly critical in modelling hybrid (with thermal methods) or solvent retrieval applications since the phase-change of injected and originally in place fluids plays an important part in controlling the efficiency of these applications.

The objective of this paper was to experimentally investigate the vapour pressure of propane in different capillary models and compare the outcomes with computed vapour pressures from the Kelvin equation. The vapour and condensation pressures of propane were measured by using Hele-Shaw cells, capillary tubes, and homogenous/heterogeneous micromodels with various pore throat and grain sizes. As a more realistic porous media representation, rock samples such as sandstones, carbonates, and shales were also considered and the vapour pressure of propane was measured in those samples to obtain a wider perspective of how vaporization and condensation of propane occur in various capillary media with dissimilar surface properties

and porous structures. Furthermore, the results with rock samples were compared with outcomes obtained from Hele-Shaw and micromodel glass chips.

Background

Kelvin and Thomson equations are theoretical modelling approaches that describe the influence of curvature radius at vapour-liquid interface on saturation pressures and boiling points. The Kelvin equation can be expressed as

$$P_r = P_\infty \exp\left[\frac{2\,\sigma\,v^L}{r\,R\,T}\right]$$

where T is temperature, R is universal gas constant, r is droplet (or capillary) radius, v^L is molar volume of the liquid, σ is surface tension, P_∞ is vapor pressure at flat surface, and P_r is vapor pressure at curved interface. When the medium is liquid wet (concave curvature), vapour pressure of the liquid reduces with the reduction of pore size which leads the vapour pressure at confined spaces P_r to be lower than the vapour pressure at the flat surface P_∞. Similarly, liquids in tight (microscale) or extended confined (nanoscale) media sizes tend to have boiling points lower than their normal boiling temperatures at bulk conditions owing to the change of pressure drop at the gas-liquid interface and surface tension. The Thomson equation defines this phenomenon with the following equation

$$T_r = T_\infty \exp\left[-\frac{2\,\sigma\,v^L}{r\,\Delta H_{vap}}\right]$$

where ΔH_{vap} is heat of vaporization of liquid, v_L is molar volume of liquid, r is droplet (or pore radius), σ is liquid surface tension, T_∞ is temperature at bulk medium, and T_r is temperature at porous medium. In prior works (Al-Kindi and Babadagli, 2018, 2017), boiling temperatures of water, heptane, decane, and naphtha were investigated through visual experiments in tight spaces with various medium sizes and porous structures. The results were then compared with calculated boiling points by the Thomson equation. It was found that boiling points of liquids could be reduced by pore size even if it is 0.1 mm or less unlike the vaporization temperatures computed by the equation. Fig.1 shows boiling points of heptane, obtained from different experiments and the Thomson equation, at various pore sizes. The experiments in previous works were conducted under atmospheric pressure (≈1 atm). The investigation in this paper focused on observing the phase-alteration of propane under atmospheric temperature (≈21 °C) at different capillary medium sizes and compares our observations with the Kelvin equation.

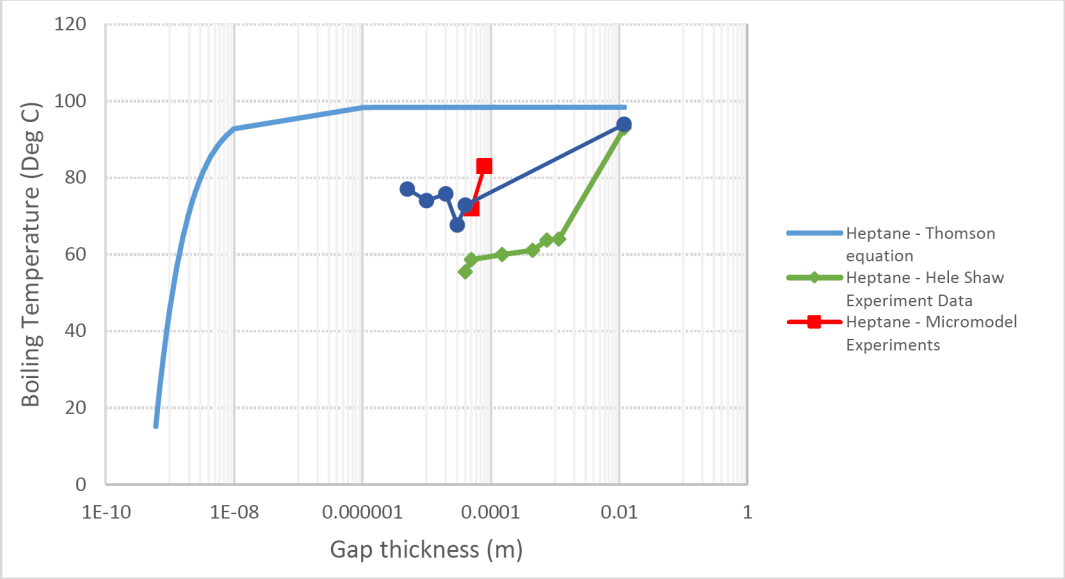

Figure 1—Boiling temperature of heptane at different pore sizes (Al-Kindi and Babadagli, 2018).

Experimental Work

Observations of propane's vaporisation and condensation pressures were performed by using several glass chips and rock samples. The experiments were initiated with Hele-Shaw glass cells of 0.13 and 0.04 mm gap thicknesses. Although the Hele-Shaw cells represent only a simple tight system with smooth and liquid-wet inner surface, they can be useful in providing a clear visualization of bubbles and drops generation of fluids in different pressures which could be difficult to visualize in microfluidic chips. Then, vapour and saturation pressures of propane were inspected in several types of micromodels with uniform and non-uniform properties such as porosity, permeability, porous structure, and pore throat/grain size. To visualize the phase change of propane in more realistic porous media, vapour pressure alteration was examined in sandstone, limestone, and shale rock samples. Using real rock samples provided an advantage of testing the impact of surface characteristics and porous media structure on vapour pressure.

Hele-Shaw Glass Cells

Hele-Shaw cells basically consist of a pair of thin rectangular glass plates with an empty gap in between. The glass cells were made with two main gap thicknesses: (1) 0.04 mm and (2) 0.13 mm. Mainly, the purpose of starting our investigation with glass cells was to get a clear exposure of propane's drops creation in pressure build-up stage and propane's bubbles formation in pressure depletion stage under constant temperature (≈21°C). In all Hele-Shaw cells, the inner glass surfaces were propane wet during condensation. Fig. 2 presents the Hele-Shaw glass cell used in our experiments.

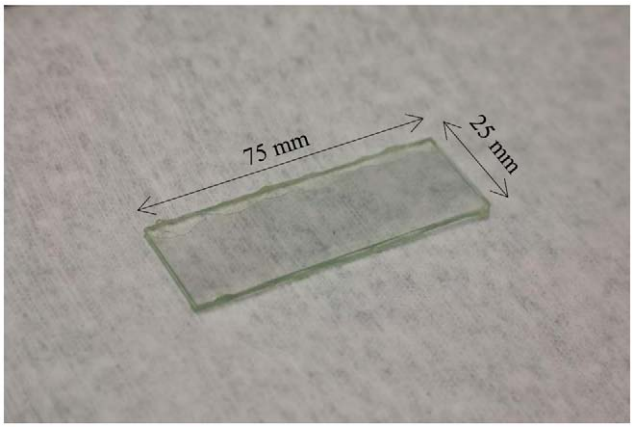

Figure 2—Hele-Shaw glass cell (0.13 mm gap thickness)

Experimental setup.. The setup consisted of a DSLR camera (Canon 7D), pressure and temperature measurement device (National Instruments), LED light source, thermocouple, pressure transducer, ISCO syringe pump, and pressure windowed cell. Fig. 3 illustrates some of the equipment used in experiments with Hele-Shaw cells.

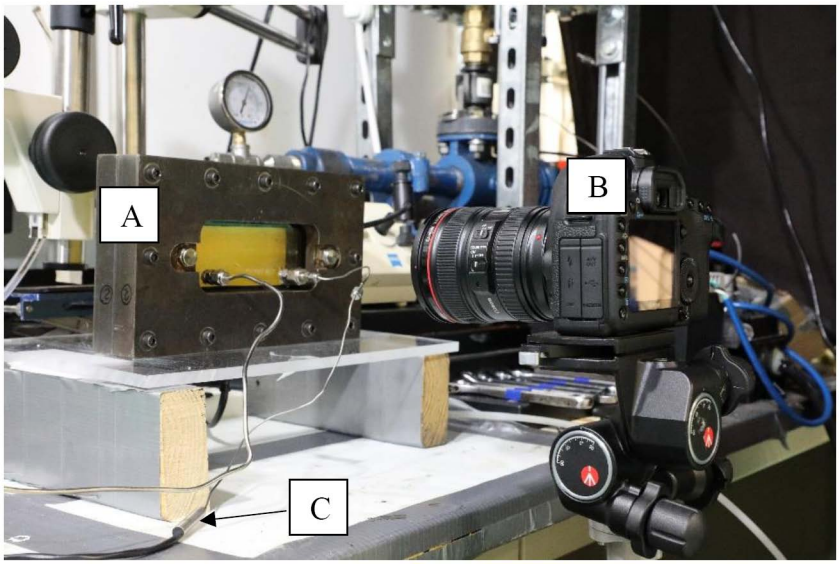

Figure 3—Experimental setup: (A) pressure windowed cell, (B) DSLR camera and (C) thermocouple.

Procedure.. To pressurize the Hele-Shaw glass models, they were placed in the pressure windowed cell. The pressure cell was featured with plexi-glass windows which allowed a clear visualization through the cell. By using an ISCO syringe pump, the cell was pressurized from a starting pressure (70 psi) to a pressure above the propane vapour pressure in Edmonton (Alberta, Canada) which was approximately 115 psi in atmospheric temperature. Both the Hele-Shaw glass cell and pressure windowed cell were vacuumed for a period of time to remove the trapped air in the system. We aimed to study both the vaporization and condensation of propane; hence, the pump was programmed to build up the pressure in the cell at a rate of 5-7 psi/min within a duration of 10 min. Likewise, to achieve the propane vaporization and determine the vapour pressure, the pump was set to deplete the pressure at a rate of 5-7 psi/min within the same duration. Meanwhile, a continuous video was taken with the DSLR camera during the process. Additionally, the pressure and temperature in the pressure cell were recorded constantly by the measurement device every two seconds.

Results and discussion.. As mentioned previously, Hele-Shaw cells provide a clearer visualization of the nucleation stage unlike microfluidic chips and rocks. Using the glass cells could bring several limitations (flat liquid-solid interface) with it which might not act as a good representation of real reservoir conditions. However, they could be useful in illustrating the phenomena under the simplest conditions. It was expected that the vapour and condensation pressure of propane in the glass cell would be relatively close to bulk pressures since their gap thicknesses were not tight enough to create effective changes in surface tension (γ) and contact angle ($\cos\theta$). During the condensation process, propane went through two main stages: (1) dew point and (2) considerable phase change. In vaporization process, two stages were considered: (1) bubble point and (2) quick formation of bubbles. In the Hele-Shaw cell with 0.04 mm gap thickness, the first propane liquid drops took place at 118.5 psi as shown in Fig. 4. A considerable phase change initiated in the cell at a pressure of 121.2 psi (Fig. 5). In the pressure depletion stage, the first propane bubbles generation took place at 116.6 psi as illustrated in Fig. 6. A quick formation of propane bubbles began in the glass cell at 113.7 psi (Fig. 7). Fig. 8 and 9 show the pressures at each stage in 0.04 mm and 0.13 mm gap spaces during pressure build-up and depletion processes.

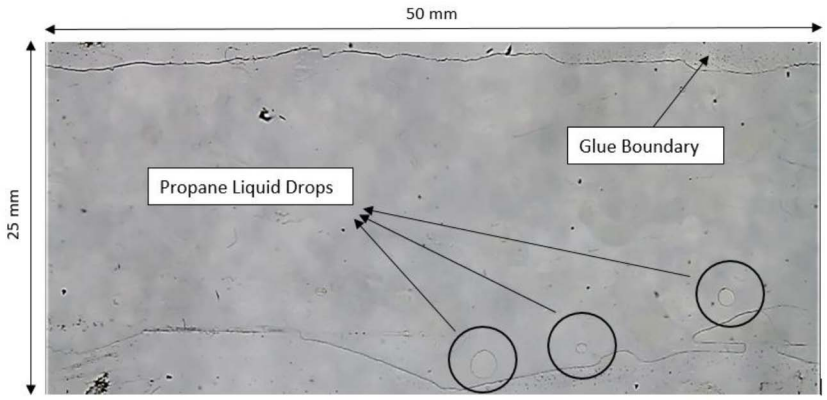

Figure 4—Dew point stage at 118.5 psi.

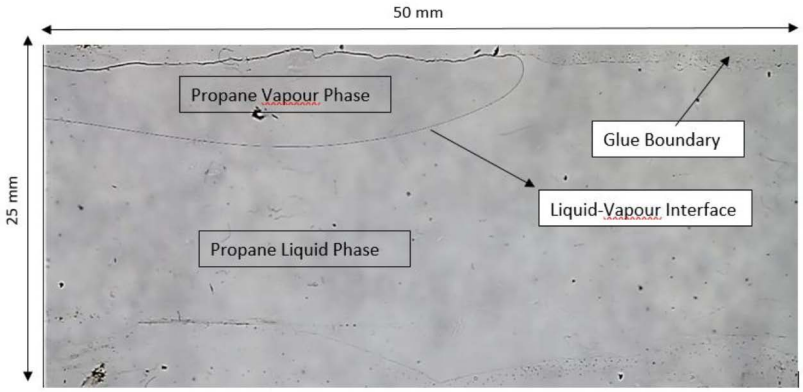

Figure 5—Considerable phase change at 121.2 psi.

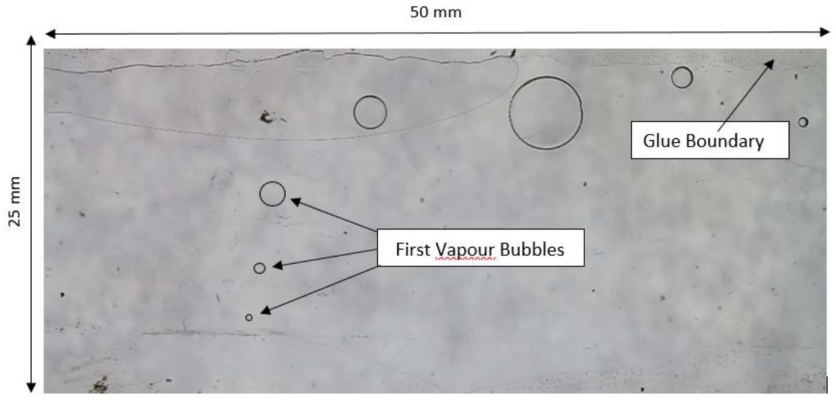

Figure 6—Bubble point stage at 116.6 psi.

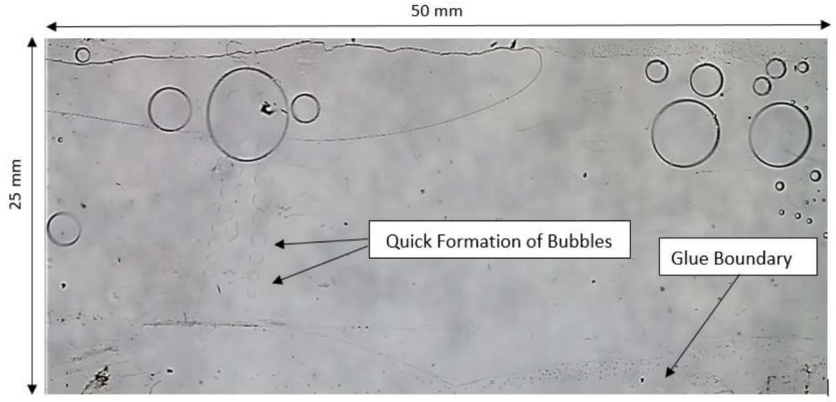

Figure 7—Quick formation of bubbles stage at 113.7 psi.

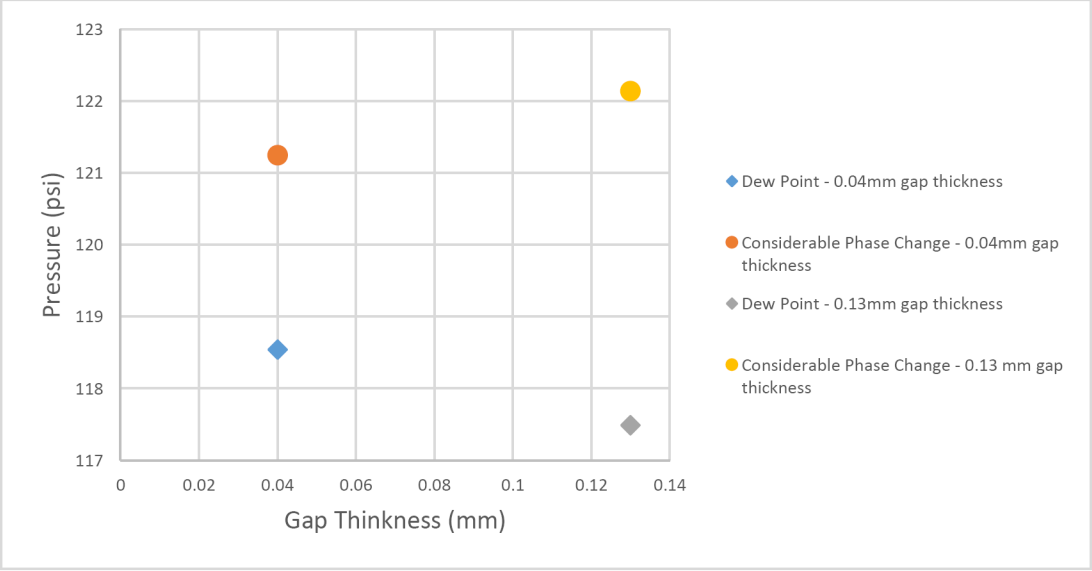

Figure 8—pressure at each stage in 0.04 and 0.13 mm gap thickness during pressure build-up process.

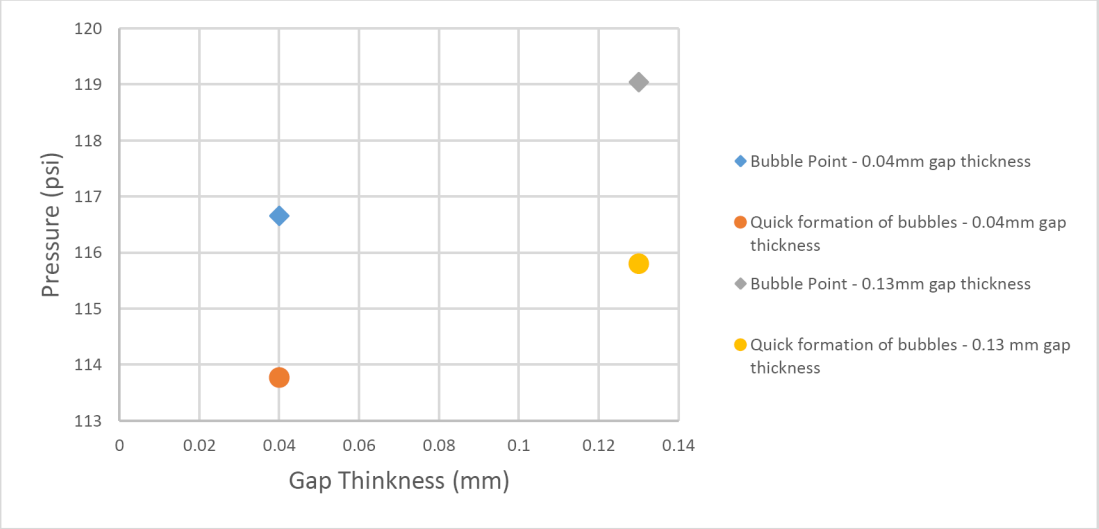

Figure 9—Pressure at each stage in 0.04 and 0.13 mm gap thickness during pressure depletion process.

Microfluidic Chips

Compared to Hele-Shaw glass cells, micromodels offer a better representation of porous media in terms of size and shape of the pores. Three categories of microfluidic chips were used: (a) capillary tube model (Fig. 10a), (b) homogenous micro model (Fig. 10b) and (c) heterogeneous micro model (Fig 10c). Capillary tubes represented straight silica-glass pore throats with various sizes ranging from 40 to 1 μm. Homogenous micromodels were designed with uniform grain and pore throat sizes. In our experiments, two homogeneous models with different properties were utilized: (1) microfluidic model with uniform properties of 0.11 mm pore diameter and 0.01 mm pore throat and (2) model with uniform properties of 0.21 mm pore diameter and 0.01 mm pore throat. Heterogeneous microfluidic chip had a porous structure closer to real rocks with an average pore throat of 142.5 μm.

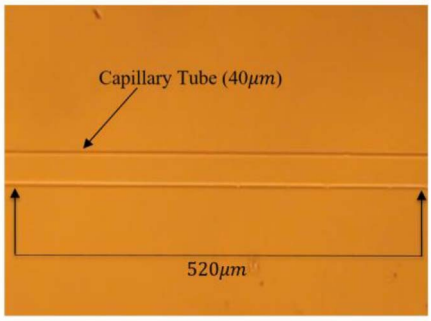

Figure 10a—40 μm capillary tube model;

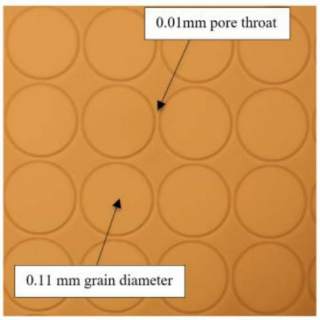

Figure 10b—Micromodel with uniform properties (0.11 mm pore diameter and 0.01 mm pore throat);

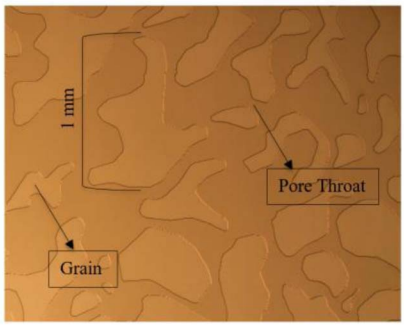

Figure 10c—Micromodel with non-uniform properties.

Experimental setup.. The setup consisted of a DSLR camera (Canon 7D), Zeiss Stemi 2000C microscope, pressure and temperature measurement device (National Instruments), LED light source, thermocouple, pressure transducer, ISCO syringe pump, and pressure windowed cell.

Procedure.. The procedure of pressurizing the micromodels was similar to the Hele-Shaw experiments. The pressure rates in the pressure build-up and depletion process were the same as the rates used in previous experiments with glass cells (5-7 psi/min). The pressure windowed cell and microfluidic chips were vacuumed for one hour to remove the trapped air. All the experiments were performed entirely under atmospheric temperature (~21°C). A continuous recording of pressure and temperature was managed during the build-up and depletion processes.

Results and discussions.. The micromodel experiments were initiated with capillary tube models featured with five sizes: (a) 40 μm, (b) 20 μm, (c) 10 μm, (d) 5 μm, and (e) 1 μm. Through capillary tube experiments, it was noticed that liquid propane wets the inner surfaces of the tubes at condensation pressures, which makes these models act as a propane-wet capillary media. In the 40 μm tube, propane started to condense at a pressure of 118.2 psi as shown in Fig. 11. During pressure depletion process, vaporization of propane took place in the tube at 116.1 psi. Table 1 shows the vaporization and condensation pressures of propane in various sizes of capillary tube during the build-up and depletion processes.

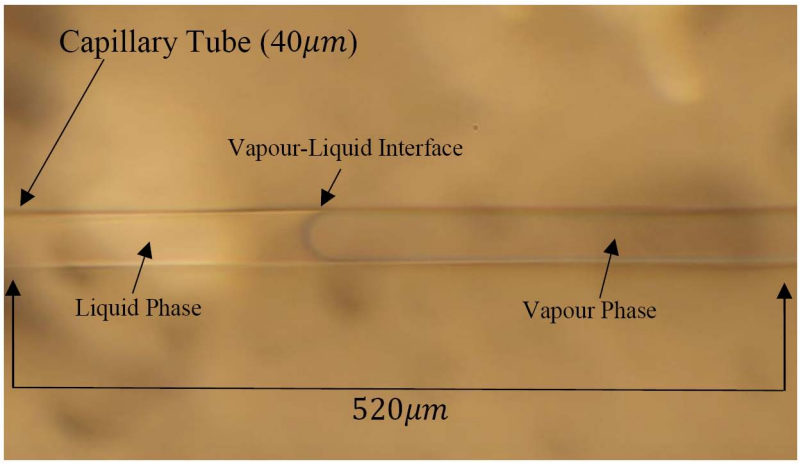

Figure 11—Propane condensation in 40 μm capillary tube.

Table 1—Vapour and saturation pressures at several capillary tube sizes.

	Vaporization pressure (psi)	Condensation pressure (psi)
40 μm Capillary tube	116.1	118.2
20 μm Capillary tube	113	121.3
10 μm Capillary tube	120.1	116.6
5 μm Capillary tube	116.1	123
1 μm Capillary tube	121.3	121.5

In microfluidic homogenous chips, phase-change pressures were relatively similar to those observed with capillary tube models. In the homogenous model (0.11 mm grain diameter and 0.01 mm pore throat), propane condensation began at 119 psi as illustrated in Fig. 12. At a pressure of 115.3 psi, vapour pressure of propane was achieved in the micromodel. Comparably, propane condensation took place in the heterogonous microfluidic model at 119.1 psi (Fig. 13). Table 2 presents the propane vaporization and condensation pressures in homogenous and heterogonous models.

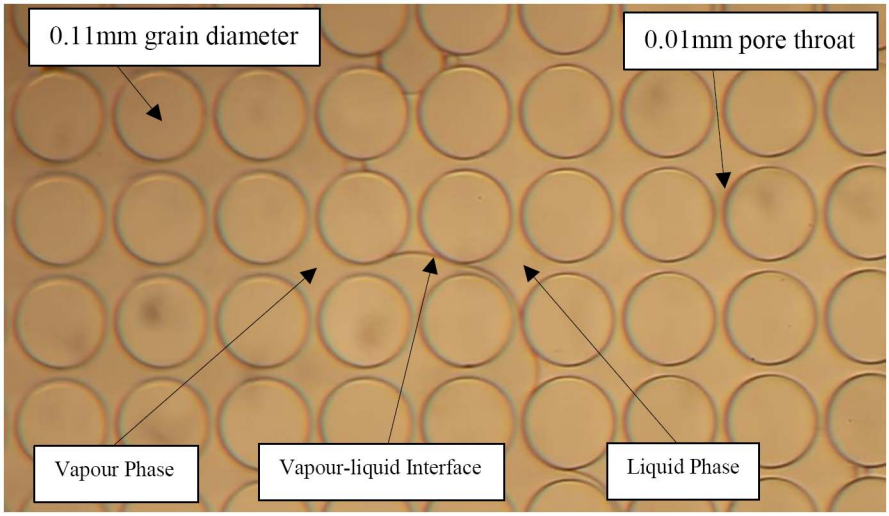

Figure 12—propane condensation in homogenous micromodel (0.11 mm grain diameter and 0.01 mm pore throat).

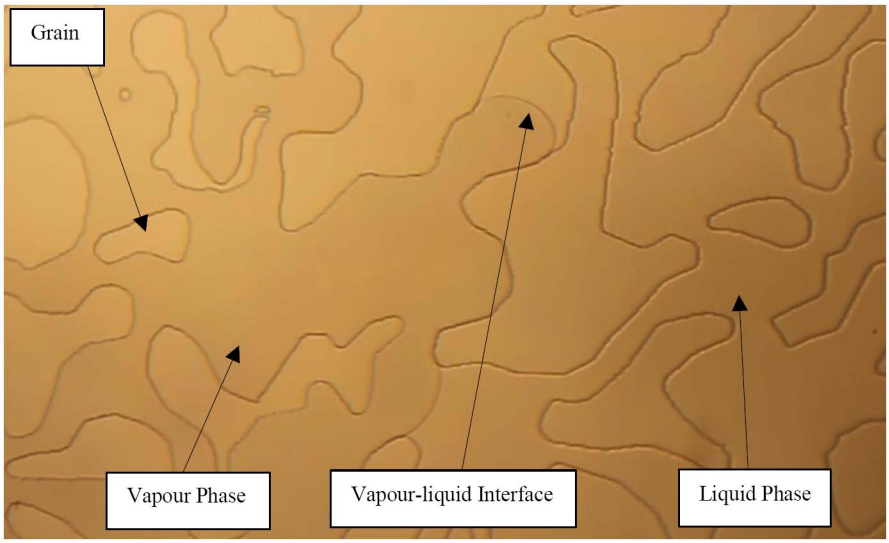

Figure 13—Propane condensation in heterogeneous micromodel (average pore throat size of 142.5 µm).

Table 2—Vapour and saturation pressures in homogenous and heterogonous microfluidic models.

	Vaporization pressure (psi)	Condensation pressure (psi)
Homogenous model (0.11 mm grain diameter and 0.01 mm pore throat)	115.3	119
Homogenous model (0.21 mm grain diameter and 0.01 mm pore throat)	117	118
Heterogeneous model (average pore throat size of 142.7 μm)	118.8	119.1

Rock Sample Experiments

To observe a more realistic observation of propane phase-change behavior in capillary (porous) media, rock samples with dissimilar properties were used. Fig. 14a – 14c show the sandstone, limestone, and shale samples before the saturation process. Table 3 illustrates permeabilites and average pore throat sizes of the core samples used in the experiments. Due to their different surface properties and pore structures, it was expected that vapour and condensation pressures might alter comparing with those observed in Hele-Shaw cells and microfluidic silica-glass chips.

Figure 14a—Limestone core sample;

Figure 14b—Sandstone core sample;

Figure 14c—Shale core sample.

Table 3—Permeability range of used rock samples.

	Limestone	Sandstone	Shale
Permeability Range (mD)	27 - 33	274	<0.01
Average Pore Throat size (μm)	7.68	22.8	0.052

Experimental Setup.. The setup consisted of a DSLR camera (Canon 7D), pressure and temperature measurement device (National Instruments), LED light source, thermocouple, pressure transducer, ISCO syringe pump, and pressure glass vessel. Fig. 15 illustrates some of the equipment used in experiments with rock samples.

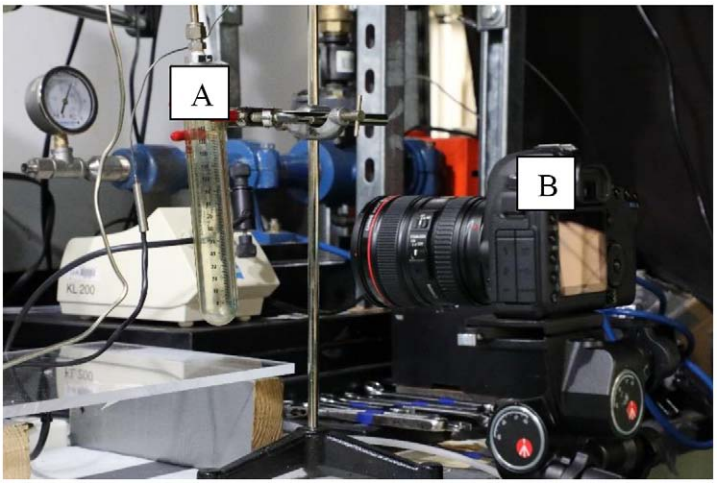

Figure 15—Experimental setup: (A) pressure glass vessel and (B) DSLR camera.

Procedure.. In rock sample experiments, only a single pressure depletion process was performed for each rock type. To eliminate the trapped air in the rock samples, the whole system was kept under vacuum pressure for one day. After that, the glass pressure vessel, including the core sample, was pressurized with propane until the condensation pressure was achieved. The system was left under pressure (~125 psi) for one day to ensure a maximum saturation of liquid propane in the rock. While performing the experiments, the vessel pressure was depleted with a rate of 5-7 psi/min. Both propane pressure and temperature were recorded continuously during the process every two seconds along with the video which was taken with the DSLR camera.

Results and discussion.. Propane in the rocks tended to vaporize at pressures lower than propane's vapour pressure at bulk conditions. For instance, in shale, propane started to change into gas phase at a pressure of 106.6 psi as presented in Fig. 16. Similarly, vapour pressures in sandstone and limestone were 10% lower than those in bulk cases. Table 4 shows the vapour pressure of propane in each rock type used in the experiments.

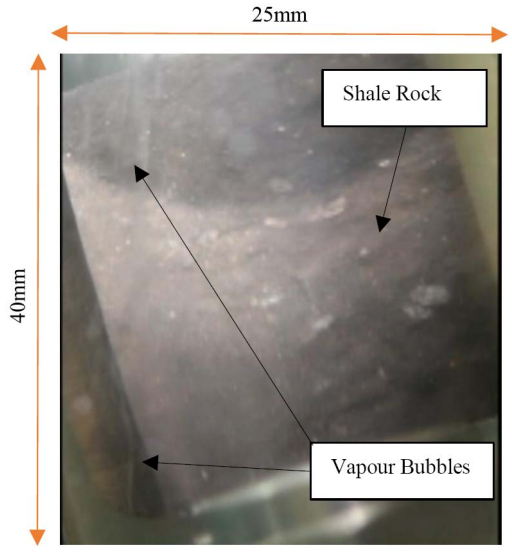

Figure 16—Propane vaporization in shale core sample.

Table 4—Propane vapour pressure in limestone, sandstone, and shale.

	Limestone	Sandstone	Shale
Vapour Pressure (psi)	104.8	103.2	106.6

Quantitative analysis

Per the Kelvin equation, vapour pressure could be altered by medium size if it is 100 *nm* or less. The vaporization pressure gets lower as the pore throat gets tighter in size. The bulk vapour and saturation pressures of propane were measured under lab conditions and phase-change, in both pressure build-up and depletion processes, of which took place at approximately 115 psi. In Hele-Shaw and microfluidic experiments, the recorded vapour and condensation pressures were relativity close to the phase-change pressures measured in bulk condition. However, with rock samples, the vapour pressures were noticed to be lower than those measured in bulk cases. Fig. 17 and 18 show the vapour and condensation pressures of propane measured in Hele-Shaw cells, micromodels, and rock samples.

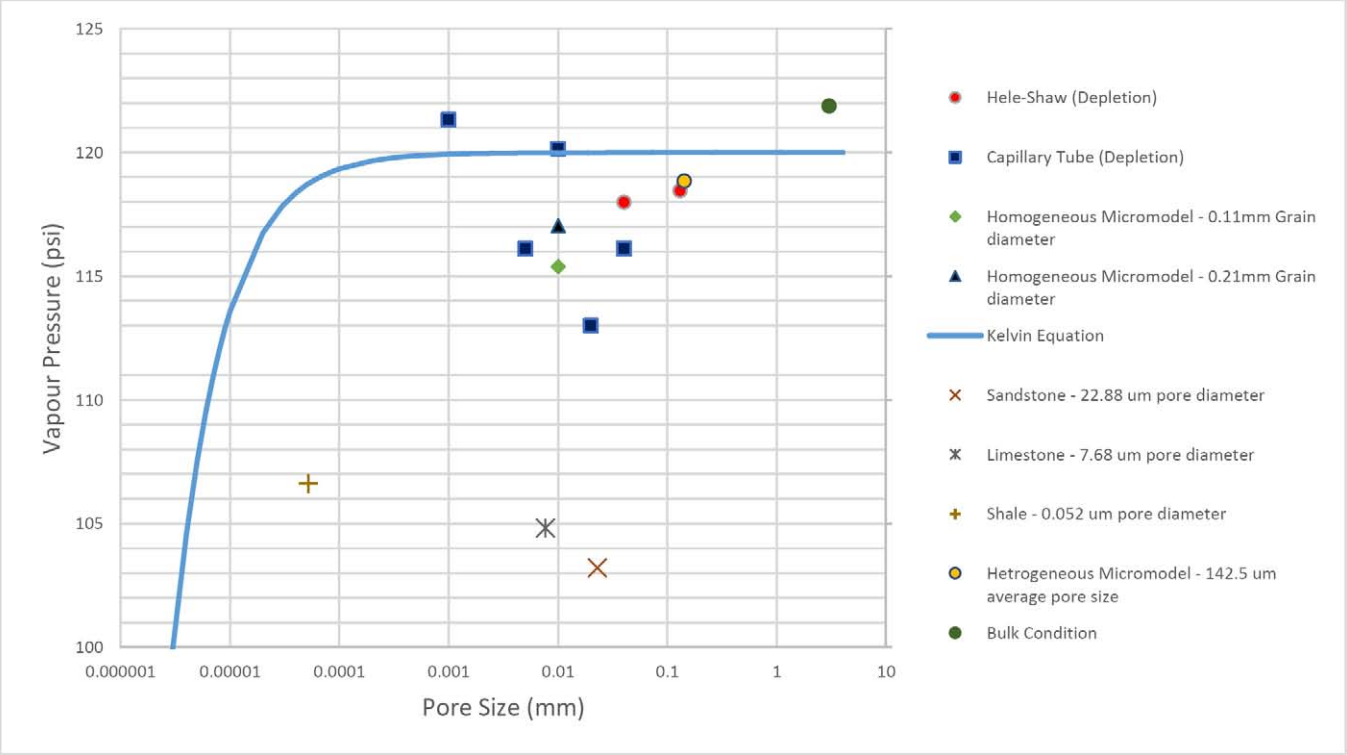

Figure 17—Vapour pressures of propane in Hele-Shaw cells, micromodels, and rock samples during the pressure depletion process.

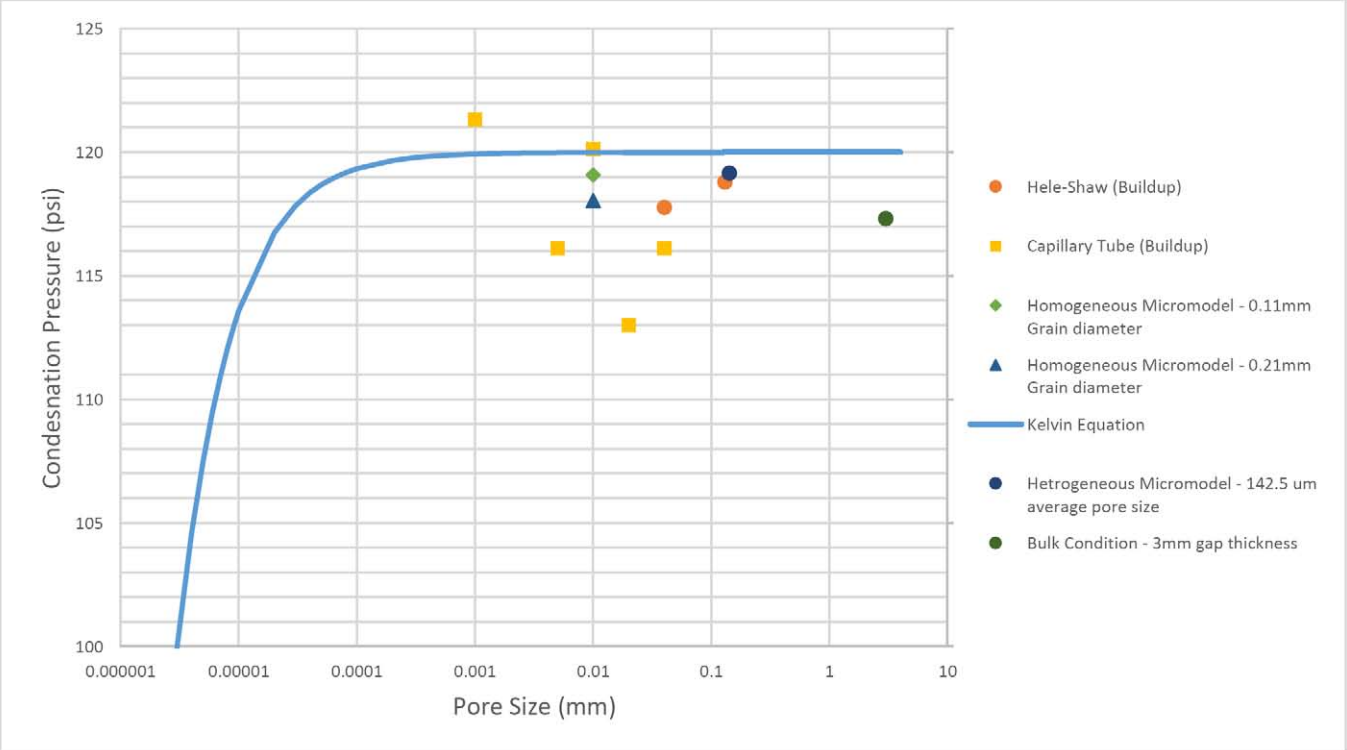

Figure 18—Saturation pressures of propane in Hele-Shaw cells, micromodels, and rock samples during the pressure build-up process.

Conclusions and Remarks

Surface characteristics of the medium including capillary size, surface tension, and curvature of vapour-liquid interface play an important role in controlling the thermodynamics and phase-alteration behaviour of liquids and gases. In order to achieve an accurate modelling of hybrid (with thermal) applications and sole solvent injection processes for oil recovery (and solvent retrieval), it is critical to understand the thermodynamics of the injected fluids (solvents) and originally-existed fluids (heavy-oil, oil, condensate) in capillary medium conditions. The main objective of this paper was to compare our experimental observations with calculated vapour pressures by the Kelvin equation. Condensation and vapour pressures of propane were investigated in capillary/porous media by using Hele-Shaw glass cells, microfluidic silica-glass chips, and rock samples. The vaporization and condensation pressures, measured at bulk condition, were considered as a benchmark and compared with phase-change pressures obtained in the experiments. Vapour and saturation pressures measured with Hele-Shaw cells and microfluidic chips were comparable with those measured at bulk conditions and computed by the Kelvin equation. Nonetheless, propane vaporized in rock samples at pressures lower than the bulk vapour pressure. The phenomena of phase alteration of propane in rocks can be explained by performing further investigations in the change of interfacial tension and contact angle as well as the effect of rock characteristics (pore structures, clay contents, etc.) on surface absorption.

Acknowledgements

This research was conducted under the second author's (TB) NSERC Industrial Research Chair in Unconventional Oil Recovery (industrial partners are Petroleum Development Oman, Total E&P Recherche Development, SIGNa Oilfield Canada, Husky Energy, Saudi Aramco, Devon, APEX Eng., and BASF) and an NSERC Discovery Grant (No: RES0011227). We gratefully acknowledge these supports. The first author (IK) is thankful to Petroleum Development Oman Co. (PDO) for providing the financial support for his graduate study at the University of Alberta. He would like also to acknowledge Dr. Al-Muatasm Al-Bahlani of PDO (Habhab Field Project Manager) for his thoughtful comments.

Nomenclature and abbreviations

EOR – Enhanced Oil Recovery
SOS-FR - Steam-Over-Solvents in Fractured Reservoir
CSS - Cyclic Steam Stimulation
SRP – Solvent Retrieval Process
v^L : liquid molar volume $[m^3/mol]$
r : droplet radius $[m]$
R : universal gas constant $\left[\frac{J}{K\ mol}\right]$
T : temperature $[K]$
P_∞ : vapor pressure at flat surface $[Pa]$
P_r : vapor pressure at curved interface $[Pa]$
T_r : temperature at porous medium $[K]$
T_∞ : temperature at bulk medium $[K]$
ΔH_{vap} : heat of vaporization $[J/mol]$

References

Al-Bahlani, A. M. M. and Babadagli, T., 2009. Laboratory and Field Scale Analysis of Steam Over Solvent Injection in Fractured Reservoirs (SOS FR) for Heavy Oil Recovery. SPE Annual Technical Conference and Exhibition, New Orleans, Louisiana, 4-7 October. SPE-124047-MS. https://doi.org/10.2118/124047-MS.

Al-Kindi, I. and Babadagli, T. 2018. Thermodynamics of Hydrocarbon Solvents at the Pore Scale During Hybrid Solvent-Thermal Application for Heavy-Oil Recovery. SPE EOR Conference at Oil and Gas West Asia, Muscat, Oman, 26-28 March. SPE-190469-MS. https://doi.org/10.2118/190469-MS.

Al-Kindi, I. and Babadagli, T. 2017. Revisiting Thomson Equation for Accurate Modeling of Pore Scale Thermodynamics of Hydrocarbon Solvents. SPE Annual Technical Conference and Exhibition, San Antonio, Texas, 9-11 October. SPE-187384-MS. https://doi.org/10.2118/187384-MS.

Bao, B., Zandavi, S. H., Li, H. et al 2017. Bubble nucleation and growth in nanochannels. *Phys. Chem. Chem. Phys.* **19**, 8223–8229. https://doi.org/10.1039/c7cp00550d.

Léauté, R. P. and Carey, B. S. 2007. Liquid Addition to Steam for Enhancing Recovery (LASER) of bitumen with CSS: Results from the first pilot cycle. *J. Can. Pet. Technol*. **46**(9): 22–30. PETSOC-07-09-01. https://doi.org/10.2118/07-09-01.

Nasr, T. N., Beaulieu, G., Golbeck, H. et al 2003. Novel Expanding Solvent-SAGD Process "ES-SAGD." *J. Can. Pet. Technol*. **42**(1): 13–16. PETSOC-03-01-TN. https://doi.org/10.2118/03-01-TN.

Tsukahara, T., Maeda, T., Hibara, A. et al 2012. Direct measurements of the saturated vapor pressure of water confined in extended nanospaces using capillary evaporation phenomena. *RSC Adv.* **2**, 3184–3186. https://doi.org/10.1039/c2ra01330d.

Zhong, J., Riordon, J., Zandavi, S. H. et al 2018. Capillary Condensation in 8 nm Deep Channels. *J. Phys. Chem. Lett.* **9**(3): 497–503. https://doi.org/10.1021/acs.jpclett.7b03003.